Demonstration of slow sound propagation and acoustic transparency with a series of detuned resonators

Arturo Santillán* and Sergey I. Bozhevolnyi
Department of Technology and Innovation, University of Southern Denmark, Niels Bohrs Allé 1, 5230 Odense M, Denmark
(Received 2 July 2013; revised manuscript received 22 April 2014; published 5 May 2014)

We present experimental results demonstrating the phenomenon of acoustic transparency with a significant slowdown of sound propagation realized with a series of paired detuned acoustic resonators (DAR) side-attached to a waveguide. The phenomenon mimics the electromagnetically induced transparency in atomic physics. By arranging four identical DAR pairs along the waveguide with an equal subwavelength separation between adjacent pairs, we show that this arrangement features unique properties of narrow-band transmission and strong dispersion. In particular, we demonstrate side-lobe suppression of more than 20 dB on both sides of the transparency window, and we quantify directly (using a pulse propagation) the acoustic slowdown effect, resulting in the sound group velocity of ∼9.8 m/s (i.e. in the group refractive index of 35). We find very similar values of the group refractive index by using measurements of the phase of the transmitted wave. It is also shown that a direct coupling exists between the DAR in each pair, which cannot be explained by the interference of waves radiated from those resonators. This detrimental coupling becomes noticeable for small values of detuning and also if the cross-sectional area of the neck of the resonators is increased.

DOI: 10.1103/PhysRevB.89.184301 PACS number(s): 43.35.+d, 43.20.+g, 42.50.Gy

I. INTRODUCTION

In the phenomenon of electromagnetically induced transparency (EIT), an opaque medium exhibits enhanced transmission in a narrow frequency window along with strong dispersion. The phenomenon involves the laser-induced coherence of atomic states leading to quantum interference between the excitation pathways controlling the optical response [1]. An interesting characteristic of EIT is the significant slowdown of light propagation due to a strong dispersion; an experimental demonstration of quantum EIT produced the propagation of optical pulses at 20 million times slower than the speed of light in vacuum [2]. Realization of EIT-like response with classical oscillator systems has been reported for a large number of photonic and plasmonic configurations (see Ref. [3] and recent reviews [4,5]). A phenomenon mimicking the EIT has also been produced in acoustics, but considerable less attention has been paid, and most of the work has been devoted to theoretical investigations. Electromagnetically induced transparency-like behaviors in acoustics have been theoretically predicted considering different systems, namely using distant coupling of two resonators grafted along a tube and separated by a distance of about one wavelength [6] (similar to the coupled resonator-induced transparency known in photonics [7]), by means of sonic crystals [8], and by utilizing differently oriented rod resonators with highly different quality factors [9], which is in a complete analogy with the plasmon-induced transparency by near-field coupled radiative and subradiant (dark) plasmonic elements [10].

Electromagnetically induced transparency-like responses and transmission spectra have been observed with different optical metamaterials [4,5,10–13]. These artificial materials have the potential of controlling wave propagations in the subwavelength scale. As their optical counterparts, acoustic metamaterials exhibit several extraordinary properties not found in nature, for example, negative bulk modulus and mass density [14–18], and negative refractive index [19–21]. Furthermore, fascinating effects have been produced such as acoustic cloaking [22–25], subwavelength focusing [26–29], and subwavelength imaging [30–34].

In a previous paper [35], we considered an acoustic phenomenon that mimics the transmission peak in the EIT, which is realized as the doublet of dressed states produced by the cancelation of opposite contributions from two different resonances due to the Fano-like interference of the decay channels, which has been also investigated for electromagnetic waves [1,11,36,37]. The two resonances were equally spaced but with opposite signs of detuning from the probe frequency. We theoretically studied the transmission of sound through a waveguide with a series of pairs of side-branch detuned acoustic resonators (DAR). Resonators forming one DAR pair were located at the same axial position along the waveguide constituting a unit referred to hereafter as a cell. Importantly, such cells were equally spaced from one another along the waveguide at a subwavelength interval. We theoretically showed that the arrangement of DAR pairs can be considered as a one-dimensional (1D) acoustic metamaterial with unique dispersion and filtering properties. However, our experiments as well as another very similar experiment [38] were carried out using only one DAR pair attached to the waveguide, an arrangement that can be sufficient to observe the EIT-like transmission spectra but does not certainly allow one to demonstrate and quantify the associated slowdown effect.

In this paper, we present experimental results demonstrating, for the first time to our knowledge, the slowdown of sound propagation in an acoustic metamaterial along with the EIT-like transmission spectra. In addition, we analyze the effect of detuning of the two resonators in one cell, the coupling between the DAR pair, the coupling between different cells in the waveguide, and the consequence of increasing the cross-sectional area of the neck of the resonators.

*Corresponding author: aos@iti.sdu.dk

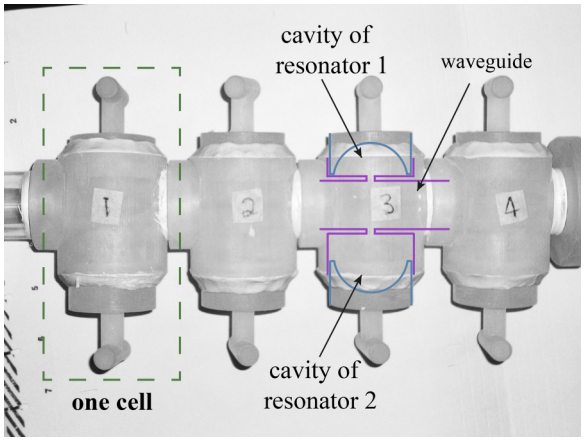

FIG. 1. (Color online) Section of the used waveguide with the series or four practically identical cells. In this arrangement, one cell contains two detuned Helmholtz resonators attached as side-branches at the same position along the axis of the waveguide; each resonator was tuned by adjusting the volume of its cavity. For the third cell from the left, the cavities of the resonators are schematically indicated in the picture.

II. EXPERIMENTAL SETUP

In the studied configuration of the acoustic 1D metamaterial, the waveguide consisted of an acrylic pipe of constant circular cross-sectional area with an inner diameter of 2 cm and with a 0.5-cm-thick wall. The whole waveguide was formed by two pipe sections, each with a length of 2 m.

A series of four practically identical cells, each formed by two DAR, was used in the experiments (Fig. 1). The 4-cell packet was placed between the two sections of acrylic pipe, i.e. in the middle along the waveguide. For the first set of experiments, the radius and the length of the neck of all the resonators were, respectively, 2.2 and 1.0 mm. The cavity of each resonator had a cylindrical shape ending by a movable piston with a semispherical inner surface. By changing the position of the piston, the volume of the cavity of each resonator was adjusted to set the desired resonance frequency.

The separation between two adjacent cells l_c was equal to 5.8 cm in all the experiments. This separation is taken as the distance along the axis of the waveguide between the centers of the openings that form the necks of the resonators in those cells. The chosen separation was a fraction of the minimum wavelength in the frequency range of interest.

The sound waves were generated by means of an electrodynamic driver for a horn loudspeaker, which had a throat with an inner diameter of 1 in at the end. The driver was attached at the beginning of the waveguide. The other end of the guide terminated in a flat rigid surface, where a pressure-field microphone of 0.5 in was placed to measure the sound pressure.

As in our case, several acoustic metamaterials have been implemented by means of arrays of Helmholtz resonators [39–42]. Interestingly, a new theoretical formulation based on an analogy between the fundamental equations of electrodynamics and acoustics has been proposed for longitudinal acoustic wave propagation in rigid-framed porous media that can be applied to acoustic metamaterials [43].

III. MATHEMATICAL MODEL

In the mathematical description, it is considered that only plane waves propagate along the waveguide. The series of Helmholtz resonators and the waveguide were mathematically described by using a lumped-parameter model and acoustic 2-port systems, which allowed a matrix formulation in terms of the number of cells (the corresponding theory has been described in our previous paper [35]). For this analytical model, it is assumed that there is no near-field coupling between individual resonators and that the cells attached to the waveguide are identical.

We consider the x direction along the axis of the pipe and assume a monochromatic incident sound wave $p_i = A_i \exp[j(\omega t - kx)]$ with angular frequency ω approaching the series of cells from the left; here, k is the wave number, and A_i is the (constant) amplitude.

The acoustic impedance (the ratio between the sound pressure and volume velocity) at the opening of the first resonator in a cell is given by $Z_1 = R_1 + j(\omega M_1 - K_1/\omega)$, where R_1, M_1, and K_1 are, respectively, the acoustic resistance, inertance, and stiffness of the resonator. Here, $M_1 = \rho L_{\mathrm{ef1}}/S_{\mathrm{res}}$ and $K_1 = \rho c^2/V_1$, where ρ is the density of the medium (air in our experiments), c is the sound speed, V_1 is the volume of the resonator, S_{res} is the cross-sectional area of the neck, and L_{ef1} its effective length. Accordingly, a similar expression describes the acoustic impedance Z_2 at the opening of the second resonator in the cell.

Let A_t denote the amplitude of the wave transmitted at the end of the cell array. We first consider only one cell in the waveguide, so that the ratio A_t/A_i (the acoustic pressure transmission coefficient) is given by the following simple expression [44]:

$$\frac{A_t}{A_i} = \frac{2Z_c}{Z + 2Z_c}, \tag{1}$$

where $Z = \rho c/S$, S is the cross-sectional area of the waveguide, and $Z_c = Z_1 Z_2/(Z_1 + Z_2)$ is the combined acoustic impedance of the two resonators.

For a periodic array of N cells, the waveguide segment that includes the Helmholtz resonators can be regarded as an acoustical 2-port system [45]. In this way, the sound pressure amplitude p_{in} at $x = 0$ (the assumed position of the first cell) and the volume velocity U_{in} at the same location can be related to the transmitted sound pressure and the corresponding volume velocity as $[p_{\mathrm{in}}\, U_{\mathrm{in}}]^{\mathrm{T}} = \mathbf{M}[A_t\, A_t/Z]^{\mathrm{T}}$, where matrix $\mathbf{M}$ is given by $\mathbf{M} = (\mathbf{M}_C\, \mathbf{M}_T)^{N-1}\mathbf{M}_C$, and

$$\mathbf{M}_C = \begin{bmatrix} 1 & 0 \\ 1/Z_C & 1 \end{bmatrix}, \qquad \mathbf{M}_T = \begin{bmatrix} \cos(kl_c) & iZ\sin(kl_c) \\ i\sin(kl_c)/Z & \cos(kl_c) \end{bmatrix}. \tag{2}$$

The acoustic pressure reflection coefficient can then be calculated [45] as $R = A_r/A_i = (Z_{\mathrm{in}} - Z)/(Z_{\mathrm{in}} + Z)$, where A_r is the complex amplitude of the wave reflected from the first cell, $Z_{\mathrm{in}} = p_{\mathrm{in}}/U_{\mathrm{in}}$. Consequently, the complex amplitudes of the incident and transmitted waves are connected with the relation $[A_t\, A_t/Z]^{\mathrm{T}} = \mathbf{M}^{-1}[(1+R)A_i\,(1-R)A_i/Z]^{\mathrm{T}}$,

from which the transmission $|A_t/A_i|^2$ for the N cells can be obtained.

IV. EXPERIMENTAL RESULTS

For the experimental determination of the transmission coefficient, a rectangular pulse with a width of 0.2 ms was produced by means of a signal generator. The pulse was amplified and fed to the electrodynamic driver. In turn, the output signal from the microphone was amplified by using a measuring amplifier. The signal from the generator and the amplified output signal from the microphone were simultaneously recorded using a sound card connected to a personal computer. A time window was used in the recorded signal from the microphone in order to eliminate the acoustic waves reflected from the section with the resonators and also from the loudspeaker.

In the first part of the process to determine the transmission as a function of frequency, the rectangular pulse was reproduced with the resonators attached to the waveguide, and the output signal from the microphone was recorded. In the second part, all the resonators were removed from the waveguide by taking out the pistons at the ends of the cavities of the resonators and filling with modeling clay the orifices in the pipe that formed the necks of the resonators. In this way, the waveguide consisted of the pipe alone, and its length was not modified. A rectangular pulse was reproduced, and the output signal from the microphone was again recorded. Thus, the transfer function between the signal recorded with the resonators attached to the waveguide and the recorded signal for the propagation in the pipe alone gives the pressure transmission coefficient as a function of frequency. Accordingly, the square of the absolute value of the pressure transmission coefficient corresponds to the (energy) transmission spectrum.

Each resonator was individually tuned by trial and error based on the experimental curve of the pressure transmission coefficient as a function of frequency obtained with the considered resonator being the only one attached to the waveguide.

The parameters for each resonator needed in the mathematical model are the volume of the cavity, the diameter and effective length of the neck, and the acoustic resistance. For the theoretical calculation of the transmission through the waveguide with four cells, it was assumed that all the cells in the arrangement were identical. In this way, only the parameters of the two Helmholtz resonators in the first cell of each arrangement were determined and used in the calculations. The diameters of the necks of the resonators were measured to calculate the cross-sectional area of the neck. The other parameters for each of the two resonators in the first cell were calculated from the transmission spectrum obtained with only the particular resonator being attached to the waveguide. Those parameters were calculated by means of Eq. (1) with Z_c equal to Z_1 or Z_2, and using the minimum value of the transmission, the frequency corresponding to that value (the resonance frequency of the resonator), and the two frequencies at which the transmission was higher than the minimum value by 3 dB.

For the first series of experiments, the necks of the resonators were constructed with a very small diameter to achieve a better correspondence to the assumptions in the theoretical model based on lumped parameters. The measured values of the diameters of the necks of the eight resonators were within the interval of 4.4 ± 0.04 mm.

However, a small cross-sectional area of the neck of the resonators in the cells increases the acoustic resistance, which has a negative effect on the transmission and on the reduction of the speed of sound. Results corresponding to a waveguide with four cells and resonators with necks of larger cross-sectional area are presented in Secs. IV C–IV E.

A. Effect of detuning

Three different arrangements containing four cells of DAR were studied and compared. The resonance frequency of the first resonator in the four cells was set to a different value in each arrangement, while the resonance frequency of the second resonator in the cells was the same for all three arrangements.

For the first waveguide, the resonance frequency of the first resonator was equal to 604 ± 4 Hz (here, 604 Hz is the average value among the four resonators of the measured resonance frequencies, and 4 Hz represents the maximum deviation of the resonance frequency from the average value). For the other two arrangements, the corresponding values were 712 ± 4 Hz and 833 ± 11 Hz, respectively. The resonance frequency of the second resonator in the cells was equal to 1112 ± 8 Hz in all arrangements. The experiments were also carried out with only one cell in each of the three different waveguides.

The interference of the two detuned resonators in the unit cells creates a narrow transmission at a frequency approximately equal to the mean value of the two resonance frequencies. The obtained experimental results show that the frequency band of the transparency window becomes smaller as the difference between the resonance frequencies of the two resonators in the cell decreases (Fig. 2). At the same time, the transmission values in the transparency window are reduced.

In addition, it can be observed that the transmission is very small on both sides of the transparency window. These two frequency intervals have a broader bandwidth, and the transmission becomes even smaller when the number of cells attached to the waveguide increases. As an example, for the arrangement number three with four cells, in which the resonance frequency of the resonators are 833 and 1112 Hz, the peak of transmission in the transparency window occurs at 970 Hz, and the transmission is very small in the band between approximately 670 and 800 Hz and also in the band between approximately 1030 and 1325 Hz. As seen in Fig. 2(b), for the waveguides with four cells, the decrease in the transmission between the maximum value in the transparency window and the side stop frequency bands was more than 20 dB.

B. Coupling between resonators

In this subsection, we show that, when the diameter of the resonators in the cells is much smaller than the wavelength and the detuning between the two resonators in each cell is large, the transparency effect and the associated dispersion in the linear array of cells in the waveguide arise only from

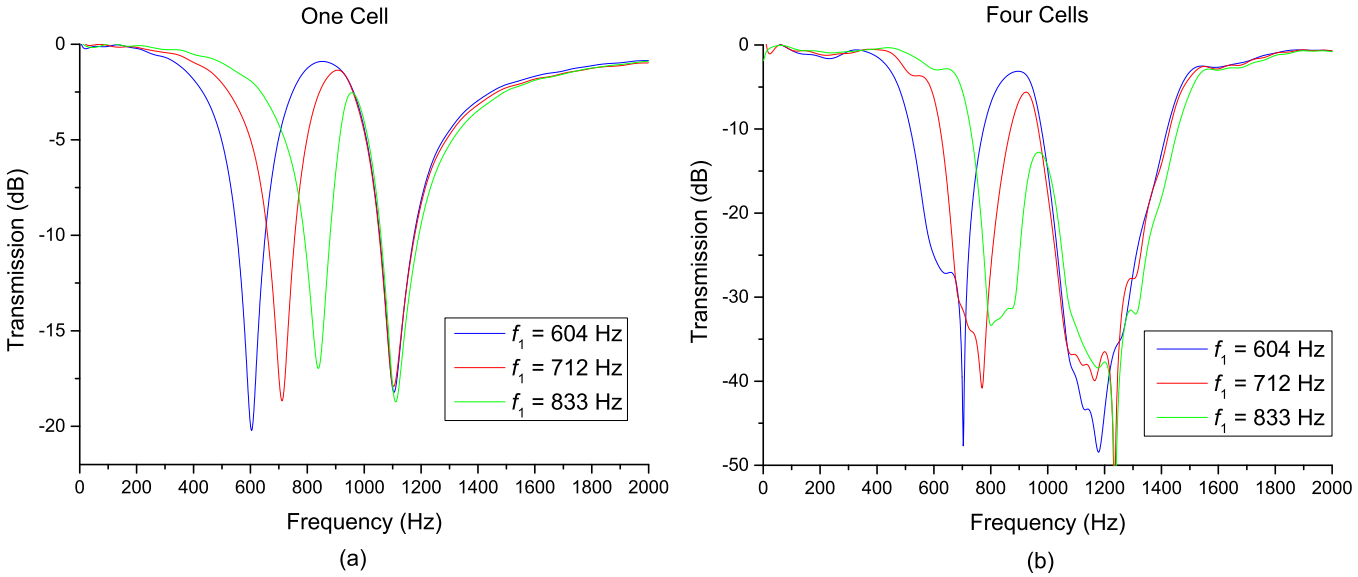

FIG. 2. (Color online) Effect of the detuning between the pair of resonators in the cells of a waveguide. (a) Transmission with only one cell in the waveguide, and (b) with four practically identical cells in the waveguide. Three different cases of detuning are compared, for which the values of the resonance frequency of the first resonator f_1 in each cell are, respectively, 604, 712, and 833 Hz, while the resonance frequency of the second resonator was adjusted to $f_2 = 1112$ Hz.

interference of radiation from DAR cells. However, if the detuning is sufficiently small, additional (coupling) effects appear that cannot be calculated using our theoretical model, which is based on the individual acoustic impedances of the resonators and the use of a transfer matrix between cells.

In the mathematical model, the two Helmholtz resonators in one cell are assumed as lumped elements characterized by the acoustic impedances Z_1 for the first resonator and Z_2 for the second one. These two resonators can be considered as being connected in parallel in an equivalent acoustical circuit. Interference is the only interaction between the two detuned resonators considered in the model.

When the experimental and the theoretical curves of the transmission versus frequency are compared, it can be observed that the section of the transmission curve corresponding to the transparency window appears more symmetric in the theoretical curve than in the experimental one. This behavior becomes apparent if the detuning between the two resonators in the cells is small. As a consequence, the peak of transmission in the experimental curve always occurs at a slightly lower frequency than the peak of the transmission for the theoretical curve.

As an example, we present in Fig. 3 the comparison between the theoretical and the experimental curves for a waveguide with one cell and also with four cells both for DAR with resonance frequencies of $f_1 = 604$ Hz and $f_2 = 1112$ Hz. This figure also includes the case in which the resonators in the cells had the resonance frequencies of $f_1 = 833$ Hz and $f_2 = 1112$ Hz. They correspond to the largest and the smallest values of detuning in Fig. 2.

There is a very good agreement between the experimental curves and the theoretical ones obtained with the model. For the experimental curve of Fig. 3(d), the group velocity in the transparency window is very small compared with the values outside that window. Thus, the time interval that the part of the wave with frequencies inside the transparency window takes to arrive from the loudspeaker to the microphone is slightly longer than the time interval that the part of the wave outside the transparency window takes to travel from the loudspeaker, reflect at the closed end and move in the opposite direction, reflect again on the membrane of the loudspeaker, and go back and arrive at the microphone for a second time. Therefore, the ripples that appear in the experimental curve of Fig. 3(d) are the effect of the reflection of the acoustic wave.

As can be seen in Figs. 3(c) and 3(d), the maximum transmission within the transparency window occurs at a slightly lower frequency in the experimental curve compared with the theoretical calculations. This difference between the experimental and the theoretical curves is practically the same for the transmission in the waveguide with one cell as for the transmission through four cells. Therefore, this frequency shift is produced by the coupling between the two resonators in each cell but not by the coupling between cells. If we take the transmission for one cell [curves in Fig. 3(c)] and raise those values to the fourth power, the resulting part of the curve in the transparency window is very similar to the corresponding curve for the transmission in a waveguide with four cells [see Fig. 3(d)]. It should be considered that not all the four cells in a waveguide are identical to one another. In addition, the background noise was a factor of random errors in the estimation of the parameters of the Helmholtz resonators and in the measurements to obtain the transmission curves.

The coupling between the two resonators in one cell is smaller when the detuning is larger. One can observe that the frequency shift at the maximum transmission of the experimental curve within the transparency window is slightly larger in Fig. 3(d) compared with the results in Fig. 3(b). In addition, the part of the experimental curve within the transparency window in Fig. 3(c) is slightly more asymmetrical

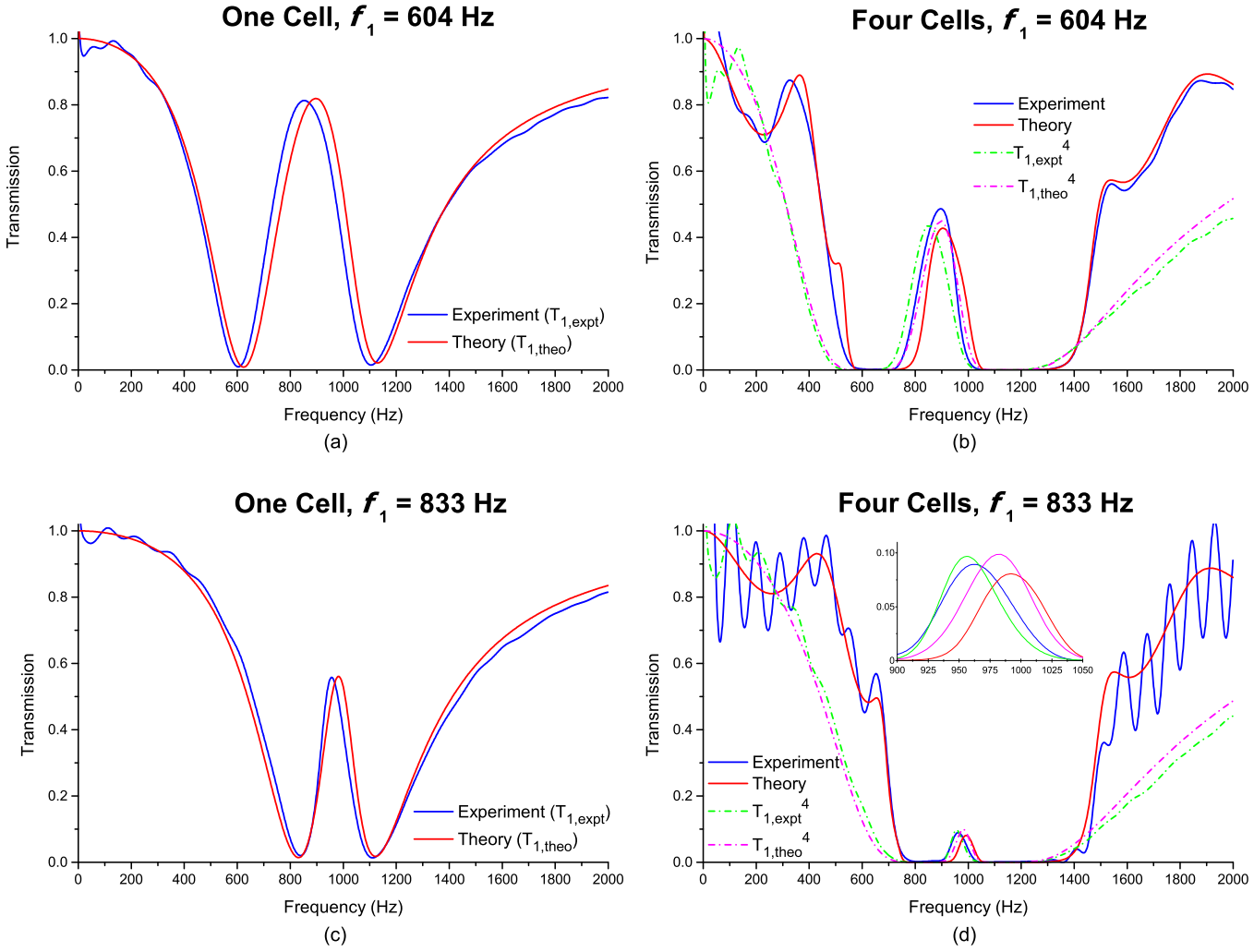

FIG. 3. (Color online) Comparison between experimental and theoretical curves of (a) transmission for a waveguide with only one cell and detuned resonators with resonance frequencies of $f_1 = 604$ Hz and $f_2 = 1112$ Hz and also (b) for a waveguide with four cells with the same detuning between the resonators. Similar graphs are presented corresponding to a smaller detuning for a waveguide (c) with one cell and (d) with four cells; the resonance frequencies of the resonators in the cells are in this case $f_1 = 833$ Hz and $f_2 = 1112$ Hz. The inset of (d) shows a closer view of the transmission in the transparency window. The values shown in (a) and (c) of the transmission for one cell are raised to the fourth power and included in the corresponding graphs for the waveguide with four cells.

than the corresponding part of the experimental curve of Fig. 3(a).

C. Effect of the neck diameter of the resonators

To decrease the acoustic resistance in the resonators, which have a negative effect on the induced transparency and on the dispersion properties of the system, the diameter of the neck of the resonators can be increased. However, as a consequence of making the opening of the resonators larger, the experimental results will deviate from the results obtained with the theoretical model.

We carried out an experiment using resonators with a neck diameter of 10.0 mm, and we adjusted the volume of those resonators to have approximately the same resonances used previously for the system with the smallest detuning shown in Fig. 2. The obtained values of the resonances were $f_1 = 831 \pm 9$ Hz and $f_2 = 1116 \pm 2$ Hz. For this case, two effects are observed in the curve of the transmission spectrum. The peak in the transparency window appears at a lower frequency in the experimental curve than the peak in the theoretical curve [Fig. 4(a)]. In addition, it can be seen that the part of the experimental curve inside the transparency window is asymmetric. These results are consistent with the observations on the curves of the transmission spectra discussed in the previous subsection. Therefore, the coupling effect between resonators in one cell that does not correspond to interference can also be increased if the diameter of the neck of the resonators is made larger.

The values of the transmission spectrum for only one cell in the waveguide are raised to the fourth power and compared with the values of the transmission for four cells in the waveguide [see Fig. 4(b)]. One can observe that the results are very similar in the frequency range of the transparency window. Thus, the maximum transmission occurs practically at the same frequency when there is only one cell or more cells

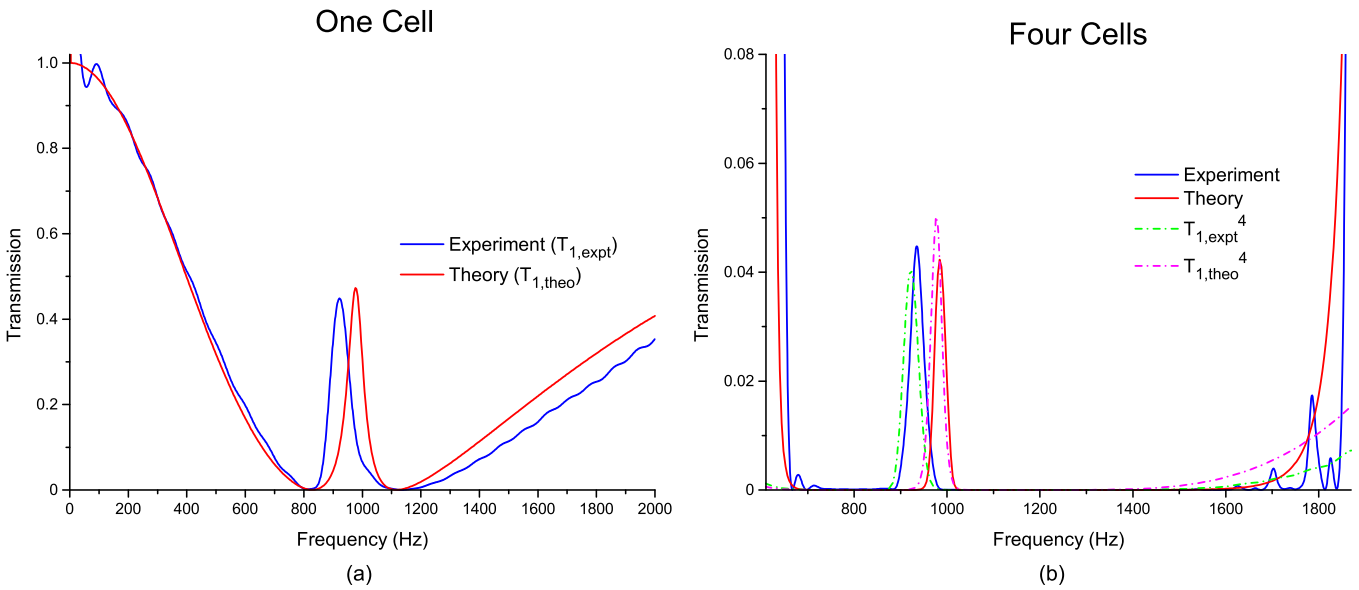

FIG. 4. (Color online) Transmission in a pipe (a) with one cell and (b) with four cells for the case in which the Helmholtz resonators in the cells have a larger neck diameter, equal to 10.0 mm. The values of the transmission for one cell shown in graph (a) are raised to the fourth power and included in graph (b).

in the pipe; the small differences are probably due to the fact that the cells are not identical. Therefore, this result can be considered as an additional indication that there is practically no coupling between the different cells for the distance of separation used between adjacent cells, even for this case in which the resonators have a larger neck diameter.

Another effect that can be observed when a larger opening in the resonators is used is the increase in the width of the stop-band regions on both sides of the transparency window. In the curves of Fig. 4(b), there is practically no transmission approximately between 725 and 900 Hz and also between 1000 and 1650 Hz. As a result, the waveguide with the four cells behaves as a good narrow band-pass filter.

By using resonators with larger diameter in the neck, the group velocity becomes even smaller in the part of the signal inside the transparency window. Therefore, in order to obtain the curve of transmission spectrum of Fig. 4(b) and the phase of the transmitted wave shown in the subsection below for this system with the larger diameter of the neck of the resonators, it was necessary to increase the length of the pipes that formed the waveguide. A section of a pipe with a length of 60 cm was inserted after the set of four cells, and another section of 20 cm was placed before the cells.

D. Slowdown of sound propagation

In this subsection, we present the results of the observed group velocity in two different waveguides each with four cells. In the first case, we used the waveguide with the smallest detuning from the three systems whose transmission spectra are shown in Fig. 2. In the second case, we used the waveguide described in the previous subsection. The main differences between the two systems are the diameter of the neck of the resonators and their volumes.

Considering the series of DAR as one-dimensional metamaterial, the effective refractive index $n(f)$ can be calculated using the following relation:

$$n(f) = -\frac{\varphi(f)}{\omega(N-1)l_c/c}, \tag{3}$$

where φ is the phase (in radians) of the transmitted wave.

In the region of normal dispersion, i.e, when $dn/df > 0$, one can determine the group refractive index $n_{\rm gr}(f)$ as follows:

$$n_{\rm gr}(f) = n(f) + f\frac{dn(f)}{df}. \tag{4}$$

The use of these two equations and the results obtained with the mathematical model give in the transparency window $n = 0.94$ and $n_{\rm gr} = 16.6$ at the frequency of 980 Hz for the series of resonators with the neck diameter of 4.4 mm. The corresponding values from the numerical calculations for the waveguide with the resonators with a neck diameter of 10.0 mm are $n = 1.16$ and $n_{\rm gr} = 45.0$ at the same frequency. Notice that the effective refractive index was very close to unity in both waveguides.

We can calculate an approximate value of the group refractive index by using the curve of the experimental phase versus frequency of the transmitted wave in the transparency window (Fig. 5). The experimental values of the phase of the transmitted wave could not be determined at the frequency intervals in which the transmission is practically zero because the signal-to-noise ratio was very small. As a consequence, the values of the experimental phase calculated in the transparency window can be different by a term of $\pm 2m\pi$ where m is an integer. Nevertheless, according to the results mentioned in the previous paragraph and Eq. (4), the group refractive index is mainly determined by the term $f(dn/df)$ since $n(f)$ is predicted to be very close to unity for the cases considered in this paper. Therefore, the relevant information here is the slope of the curve of the phase of the transmitted wave as a function of frequency.

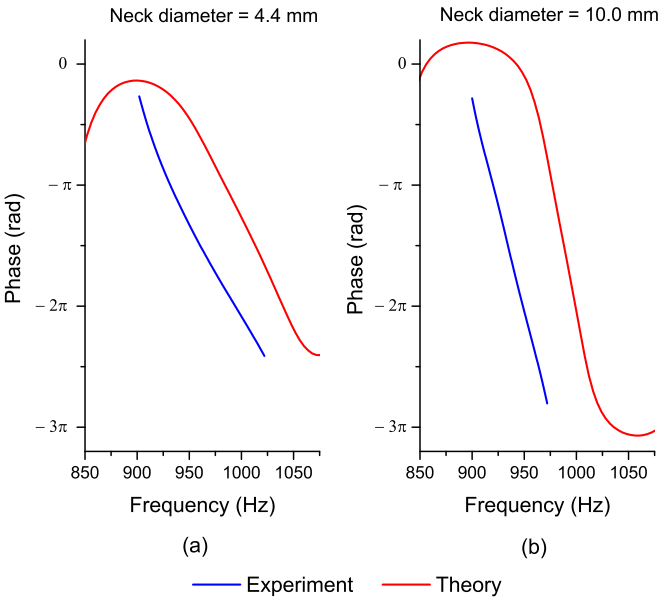

FIG. 5. (Color online) Experimental and theoretical values of the phase of the transmitted wave in the transparency window as a function of frequency for two studied waveguides each with four cells. The resonance frequencies of the detuned Helmholtz resonators in the cells were practically the same for the two waveguides, but the resonators in the first waveguide had (a) a neck diameter of 4.4 mm and a small volume compared with (b) the neck diameter of 10.0 mm and a large volume in the resonators of the second waveguide. The experimental curves have been displaced in the vertical axis to make them coincide with the theoretical results.

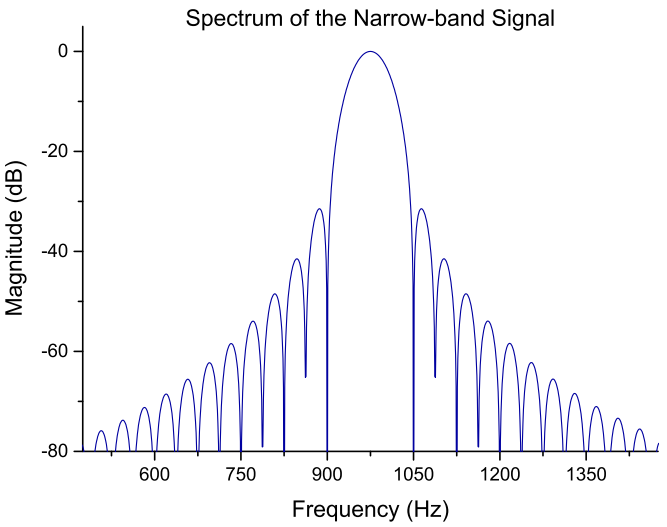

FIG. 6. (Color online) Spectrum of the computer-generated signal of short duration and narrow-band used as the input to the loudspeaker to determine the group velocity in the waveguides with four cells.

By using the points (930 Hz, −3.03 rad) and (970 Hz, −5.18 rad) on the curve of the experimental values of the phase for the waveguide with the resonators with the small neck diameter [Fig. 5(a)], we can approximate the value of $f(dn/df)$ at the frequency of 950 Hz assuming that the curve is a straight line between the two points considered. The obtained result is $n_{gr} \approx f(dn/df) \approx 15.5$. In a similar way, we can use the points (930 Hz, −4.21 rad) and (970 Hz, −8.56 rad) for the second series of resonators [Fig. 5(b)]. The result is $n_{gr} \approx 32.3$ at 950 Hz.

A very good agreement has been obtained between the values of group refractive index of the numerical simulation and the approximation from the experimental curve in the case of the resonators with the small neck diameter. However, there is a quite significant difference for the waveguide formed by the resonators with the large neck diameter. As can be seen in Fig. 5(b), this difference is also noticed in the slopes of the numerical and the experimental curves. For the results of the second waveguide, it is considered that the small value of the group refractive index compared with the value expected from the numerical calculations is due to the fact that the theoretical model based on lumped parameters assumes that the effect of the opening of the resonators does not occur in an extended region along the x direction but at a plane $x =$ constant. Thus, the bigger the diameter of the neck of the resonators, the larger the deviation from the theoretical results will be. In addition, the larger diameter also increases the direct coupling between the two DAR in one cell, as explained in the previous section.

By increasing the diameter of the neck of the Helmholtz resonators (in the presented case, the volumes of the cavities of the resonators were made larger to keep the desired resonance frequencies in the cells), the acoustic resistance of the resonators are significantly reduced. This produces a major reduction in the group velocity of the sound propagating within the transparency window.

E. Slow sound propagation with a signal of short duration

The transmission of a narrow-band signal of short duration through the waveguides with a series of four cells studied in the previous subsection and the associated slowdown in sound propagation has also been investigated. Most of the energy of the input signal to the loudspeaker was concentrated between 900 and 1050 Hz (Fig. 6), corresponding approximately to the frequency interval of the transparency window of the chain of four cells.

Here, the signal fed to the loudspeaker was generated by using the sound card connected to a computer, which was also used to record the output signal from the microphone. In this way, the recording process started at the same time as the reproduction of the narrow-band input signal.

The experiment was first carried out with the four cells attached to the waveguide, and it was repeated after the pistons at the end of the cavities of the eight resonators were removed and the orifices in pipe were blocked using modeling clay. As a result, a clear temporal delay in the propagation of the pulse along the pipe with the resonators is observed when compared with the propagation of the burst signal along the pipe without the attached resonators (see Fig. 7). The graph of the recorded signal that corresponds to the propagation through the waveguide without cells contains also a first reflection of the original reproduced signal. This reflection has been significantly attenuated by the absorption on the walls of the pipe.

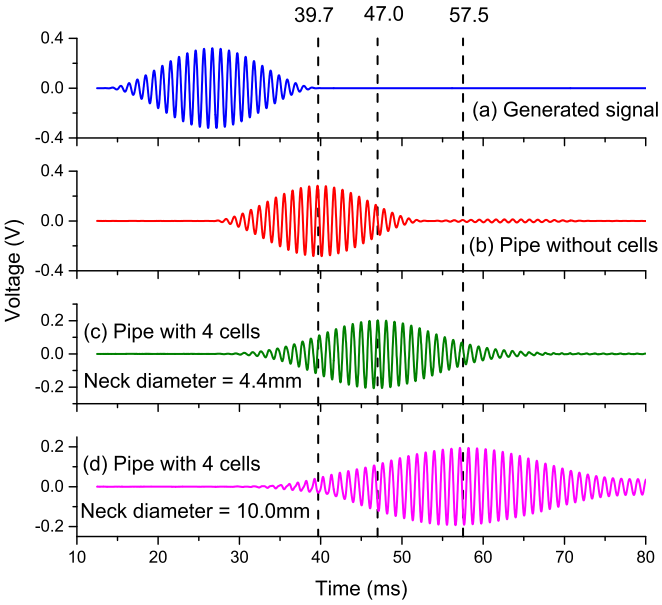

FIG. 7. (Color online) (a) Propagation of a narrow-band signal of short duration through the studied waveguide under three different conditions: (b) without the side-branched Helmholtz resonators, (c) with a series of four cells of detuned Helmholtz resonators with a neck diameter of 4.4 mm attached to the waveguide, and (d) with a new series of four cells attached to the same waveguide in which the resonators had a neck of 10.0 mm in diameter. The last three curves in the graph correspond to the output signals from the microphone at the end of the waveguide. A clear group delay is observed when sound propagated through the section with the cells. The curve of the propagation without cells has been scaled by the factor 1/3.16 for a better comparison.

As seen in Fig. 7(c), for the DAR with the neck diameter of 4.4 mm, the maximum amplitude of the envelope of the transmitted signal with the series of cells occurred at the time $t = 47.0$ ms. In comparison, the corresponding maximum of the envelope of the recorded signal in the pipe without resonators appears at the time $t = 39.7$ ms. Therefore, the distance between the first and the fourth cells, equal to 17.4 cm, was crossed by the pulse with a group delay of 7.3 ms compared with the propagation through the same distance in the pipe without resonators. The ambient temperature in the lab when the experiments were carried out was approximately 21 °C, which corresponds to a sound speed of 343.2 m/s. Hence, the group velocity with which the burst signal propagated from the position of the first cell to the position of the fourth cell is obtained by $c_g = 0.174\ \text{m}/[7.3\ \text{ms} + 0.174\ \text{m}/(343.2\ \text{m/s})]$. This gives $c_g = 22.3$ m/s, which results in a group refractive index of $n_g = 15.4$ in the section of the waveguide with the four cells.

For the case of the last curve in Fig. 7, which corresponds to the resonators with a neck diameter of 10.0 mm, the maximum value of the envelop of the burst signal occurred at the time $t = 57.5$ ms. This experiment was carried out during the summer, and the temperature in the laboratory was 26 °C. Thus, the speed of sound can be considered as 346.2 m/s. Therefore, the group velocity for the propagation of the burst signal between the first and the fourth cells was $c_g = 9.8$ m/s. This gives a group refractive index equal to $n_g = 35.3$, which is more than twice the value for the cells formed by resonators with a neck diameter of 4.4 mm. Therefore, the diameter of the neck of the resonators is a relevant factor to determine the slowdown of sound propagation.

We can see that there is a very good agreement in the values of the group velocity corresponding to the waveguide formed by the DAR with the neck diameter of 4.4 mm. The theoretical value and the experimental results obtained from the curve of the phase as a function of frequency and with the propagation of the pulse are very similar. For the waveguide with the resonators with the neck diameter of 10.0 mm, the two experimental values are very similar but smaller than the theoretical one.

It should be mentioned that the slowdown of sound propagation has also been studied in other kinds of systems, in which the physical mechanisms producing the slow group velocity are quite different from the one described in this paper. Slowdown of sound propagation has been investigated in sonic crystal waveguides [46,47] in which material parameters vary on the order of one wavelength and are a direct analogy with photonic crystals. Reported experimental results gave a group velocity of 26.7 m/s [47]. A study on the propagation of acoustic surface waves along corrugated cylindrical wires surrounded by air has theoretically shown that the group velocity can be reduced down to zero [48]. An anisotropic metamaterial made of 80 grooves perforated in a square brass alloy bar traps broadband acoustic waves and spatially separates different frequency components [49]. The effect is due to strong modulation of wave velocity through gradient subwavelength unit cells.

V. CONCLUSION

We have experimentally demonstrated that the speed of sound propagation can be significantly reduced in a 1D acoustic metamaterial by mimicking the transmission peak in the EIT. In our experiments, the metamaterial consisted of a series of four DAR pairs (cells) located as side-branches along a sound waveguide with subwavelength distance between adjacent pairs. The group refractive index was determined by means of the observed delay of the propagation of a narrow-band pulse, and also by means of the experimental data of the phase of the transmitted wave. The results were consistent between the two ways used to calculate the group refractive index in the experiments that we carried out and gave very similar values.

A very good agreement has been obtained between the experimental results and the theoretical predictions provided that the resonators satisfied the conditions of the lumped-parameter model. By using resonators with a neck of small cross-sectional area (with a diameter of 4.4 mm) to match the assumptions of the theory developed in a previous paper, we achieved a group refractive index of 15.4, which was in very good agreement with the theoretical prediction.

The presented results show that a speed of sound propagation significantly lower can be obtained in the waveguide if the acoustic resistance of the resonators is reduced by increasing the cross-sectional area of the neck of the resonators. With a waveguide formed by four DAR pairs in which the neck of

the resonators had a diameter of 10.0 mm but with the same resonance frequencies in the DAR as in the example mentioned in the last paragraph, we obtained a group refractive index of approximately 35. This particular waveguide behaved as a very narrow band pass filter with broad stop bands on both sides of the transparency window.

It has been shown experimentally that a direct coupling exists between the two DAR forming one cell, which can be observed if the cross-sectional area of the neck of the DAR is made sufficiently large. This direct coupling cannot be explained by interference. In this case, the value of the group refractive index calculated from experimental data was equal to 78% of the theoretical prediction. The experiments have shown that, when the detuning between the two acoustic resonators in a cell is small, a direct coupling also becomes apparent between the resonators. As a consequence of the coupling between the two DAR in the cells, the peak of transmission in the transparency window was observed to occur at a slightly lower frequency than the value predicted theoretically. However, in our experiments, there was no detrimental effect observed on the transmission in the transparency window produced by unexpected intercell coupling. It might be necessary to place the cells very close to one another to notice effects of coupling between them.

We believe that the reported experimental results indicate that the DAR approach does indeed offer new practical solutions for slowing down the propagation of sound waves and designing compact narrow-band acoustic transmission filters.

[1] K. J. Boller, A. Imamoglu, and S. E. Harris, Phys. Rev. Lett. **66**, 2593 (1991).

[2] L. V. Hau, S. E. Harris, Z. Dutton, and C. H. Behroozi, Nature (London) **397**, 594 (1999).

[3] X. Yang, M. Yu, D. L. Kwong, and C. W. Wong, Phys. Rev. Lett. **102**, 173902 (2009).

[4] A. E. Miroshnichenko, S. Flach, and Y. S. Kivshar, Rev. Mod. Phys. **82**, 2257 (2010).

[5] B. Luk'yanchuk, N. I. Zheludev, S. A. Maier, N. J. Halas, P. Nordlander, H. Giessen, and C. T. Chong, Nat. Mater. **9**, 707 (2010).

[6] E. H. El Boudouti, T. Mrabti, H. Al-Wahsh, B. Djafari-Rouhani, A. Akjouj, and L. Dobrzynski, J. Phys.: Condens. Matter **20**, 255212 (2008).

[7] Q. Xu, S. Sandhu, M. L. Povinelli, J. Shakya, S. Fan, and M. Lipson, Phys. Rev. Lett. **96**, 123901 (2006).

[8] J. Sánchez-Dehesa, D. Torrent, and L. W. Cai, New J. Phys. **11**, 013039 (2009).

[9] F. Liu, M. Ke, A. Zhang, W. Wen, J. Shi, Z. Liu, and P. Sheng, Phys. Rev. E **82**, 026601 (2010).

[10] S. Zhang, D. A. Genov, Y. Wang, M. Liu, and X. Zhang, Phys. Rev. Lett. **101**, 047401 (2008).

[11] S. I. Bozhevolnyi, A. B. Evlyukhin, A. Pors, M. G. Nielsen, M. Willatzen, and O. Albrektsen, New J. Phys. **13**, 023034 (2011).

[12] P. Tassin, L. Zhang, R. Zhao, A. Jain, T. Koschny, and C. M. Soukoulis, Phys. Rev. Lett. **109**, 187401 (2012).

[13] N. Papasimakis, Y. H. Fu, V. A. Fedotov, S. L. Prosvirmin, D. P. Tsai, and N. I. Zheludev, Appl. Phys. Lett. **94**, 211902 (2009).

[14] V. M. García-Chocano, R. Graciá-Salgado, D. Torrent, F. Cervera, and J. Sánchez-Dehesa, Phys. Rev. B **85**, 184102 (2012).

[15] Y. Ding, Z. Liu, C. Qiu, and J. Shi, Phys. Rev. Lett. **99**, 093904 (2007).

[16] L. Fok and X. Zhang, Phys. Rev. B **83**, 214304 (2011).

[17] M. Yang, G. Ma, Z. Yang, and P. Sheng, Phys. Rev. Lett. **110**, 134301 (2013).

[18] Z. Liang and J. Li, Phys. Rev. Lett. **108**, 114301 (2012).

[19] F. Bongard, H. Lissek, and J. R. Mosig, Phys. Rev. B **82**, 094306 (2010).

[20] Y. Xie, B.-I. Popa, L. Zigoneanu, and S. A. Cummer, Phys. Rev. Lett. **110**, 175501 (2013).

[21] J. Christensen and F. J. García de Abajo, Phys. Rev. B **86**, 024301 (2012).

[22] X. Zhou and G. Hu, Phys. Rev. E **75**, 046606 (2007).

[23] B.-I. Popa, L. Zigoneanu, and S. A. Cummer, Phys. Rev. Lett. **106**, 253901 (2011).

[24] S. Zhang, C. Xia, and N. Fang, Phys. Rev. Lett. **106**, 024301 (2011).

[25] M. Farhat, S. Guenneau, and S. Enoch, Phys. Rev. Lett. **103**, 024301 (2009).

[26] J. Christensen, A. I. Fernandez-Dominguez, F. De Leon-Perez, L. Martin-Moreno, and F. J. Garcia-Vidal, Nat. Phys. **3**, 851 (2007).

[27] F. Lemoult, M. Fink, and G. Lerosey, Phys. Rev. Lett. **107**, 064301 (2011).

[28] M. Ambati, N. Fang, C. Sun, and X. Zhang, Phys. Rev. B **75**, 195447 (2007).

[29] S. Guenneau, A. Movchan, G. Pétursson, and S. A. Ramakrishna, New J. Phys. **9**, 399 (2007).

[30] D. Lu and Z. Liu, Nat. Commun. **3**, 1205 (2012).

[31] J. Zhu, J. Christensen, J. Jung, L. Martin-Moreno, X. Yin, L. Fok, X. Zhang, and F. J. Garcia-Vidal, Nat. Phys. **7**, 52 (2011).

[32] J. S. Li, L. Fok, X. B. Yin, G. Bartal, and X. Zhang, Nat. Mater. **8**, 931 (2009).

[33] X. Y. Ao and C. T. Chan, Phys. Rev. E **77**, 025601 (2008).

[34] J. Christensen and F. J. G. de Abajo, Phys. Rev. Lett. **108**, 124301 (2012).

[35] A. Santillán and S. I. Bozhevolnyi, Phys. Rev. B **84**, 064304 (2011).

[36] Z. Han and S. I. Bozhevolnyi, Opt. Express **19**, 3251 (2011).

[37] A. Mouadili, E. H. El Boudouti, A. Soltani, A. Talbi, A. Akjouj, and B. Djafari-Rouhani, J. Appl. Phys. **113**, 164101 (2013).

[38] W. Tan, C. Z. Yang, H. S. Liu, Z. G. Wang, H. Q. Lin, and H. Chen, Europhys. Lett. **97**, 24003 (2012).

[39] N. Fang, D. Xi, J. Xu, M. Ambati, W. Srituravanich, C. Sun, and X. Zhang, Nat. Mater. **5**, 452 (2006).

[40] Z. G. Wang, S. H. Lee, C. K. Kim, C. M. Park, K. Nahm, and S. A. Nikitov, J. Phys.: Condens. Matter **20**, 055209 (2008).

[41] Y. Cheng, J. Y. Xu, and X. J. Liu, Appl. Phys. Lett. **92**, 051913 (2008).

[42] J. Fey and W. M. Robertson, J. Appl. Phys. **109**, 114903 (2011).
[43] D. Lafarge and N. Nemati, Wave Motion **50**, 1016 (2013).
[44] L. E. Kinsler, A. R. Frey, A. B. Coppens, and J. V. Sanders, *Fundamentals of Acoustics* (JohnWiley & Sons, New York, 2000), p. 291.
[45] A. D. Pierce, *Acoustics: An Introduction to Its Physical Principles and Applications* (McGraw-Hill, New York, 1981), pp. 350–354.
[46] O. A. Kaya, A. Cicek, and B. Ulug, J. Phys. D **45**, 365101 (2012).
[47] A. Cicek, O. A. Kaya, M. Yilmaz, and B. Ulug, J. Appl. Phys. **111**, 013522 (2012).
[48] J. Christensen, P. A. Huidobro, L. Martín-Moreno, and F. J. García-Vidal, Appl. Phys. Lett. **93**, 083502 (2008).
[49] J. Zhu, Y. Chen, X. Zhu, F. J. Garcia-Vidal, X. Yin, W. Zhang, and X. Zhang, Sci. Rep. **3**, 1728 (2013).